ELSEVIER

Earth and Planetary Science Letters 176 (2000) 57–72

EPSL

www.elsevier.com/locate/epsl

Recent fluid processes in the Kaapvaal Craton, South Africa: coupled oxygen isotope and trace element disequilibrium in polymict peridotites

H.-F. Zhang [a,b,*], D.P. Mattey [a], N. Grassineau [a], D. Lowry [a], M. Brownless [a], J.J. Gurney [c], M.A. Menzies [a]

[a] *Department of Geology, Royal Holloway University of London, Egham, Surrey TW20 0EX, UK*
[b] *Laboratory of Lithosphere and Tectonics evolution, Institute of Geology and Geophysics, Chinese Academy of Sciences, P.O. Box 9825, Beijing 100029, PR China*
[c] *University of Cape Town, Cape Town, South Africa*

Received 20 November 1998; received in revised form 17 November 1999; accepted 4 December 1999

Abstract

Oxygen-isotope mapping of thin sections of polymict peridotite xenoliths shows that significant oxygen isotope disequilibrium is preserved on a sub-millimetre scale in primary and secondary minerals. Primary porphyroblastic phases (e.g., olivine, orthopyroxene, garnet, diopside) tend to have higher $\delta^{18}O$ ratios than secondary minerals (e.g., mica, ilmenite, neoblastic olivine, orthopyroxene rims). Polymict minerals have a lower oxygen isotope composition than 'average mantle' ($\delta^{18}O = 5.2 \pm 0.3‰$) and show clear evidence of inter- and intra-mineral oxygen isotope disequilibrium. Disequilibrium is also evident in the elemental geochemistry of the mantle minerals and a general correlation exists between oxygen isotopes and major (Si, Mg, Ca, Fe) and trace elements (Ce, Cr, Zr, Nb, REE). The interpretation that isotopic heterogeneity may relate to melt processes is supported by $\delta^{18}O$ zonation in garnets, significant isotopic variation close to secondary veins, $\delta^{18}O$ (primary phases) $> \delta^{18}O$ (secondary phases) and oxygen isotope disequilibria in many minerals. In addition, a positive correlation between $\delta^{18}O$ and grain size indicates a role for deformation processes as a result of diffusion reactions perhaps inextricably linked to melt processes. We suggest that polymict peridotites formed as a result of movement along mantle shear zones which led to the juxtaposition of minerals of varied provenance. Contemporaneous melt transfer reacted with these mantle breccias and rapid entrainment by 'kimberlite' meant that any associated mineral disequilibrium was very effectively preserved.

Keywords: Kaapvaal Craton; diffusion; O-18/O-16; trace elements; peridotites; equilibrium

1. Introduction

The Archaean lithosphere of South Africa comprises a thick, stable mechanical boundary layer (ca 200 km) which has been affected by mantle metasomatism and/or enrichment for billions of

* Corresponding author. Fax: +86 106 2010846; E-mail: hfzhang@mail.igcas.ac.cn

0012-821X/00/$ – see front matter
PII: S0012-821X(99)00311-8

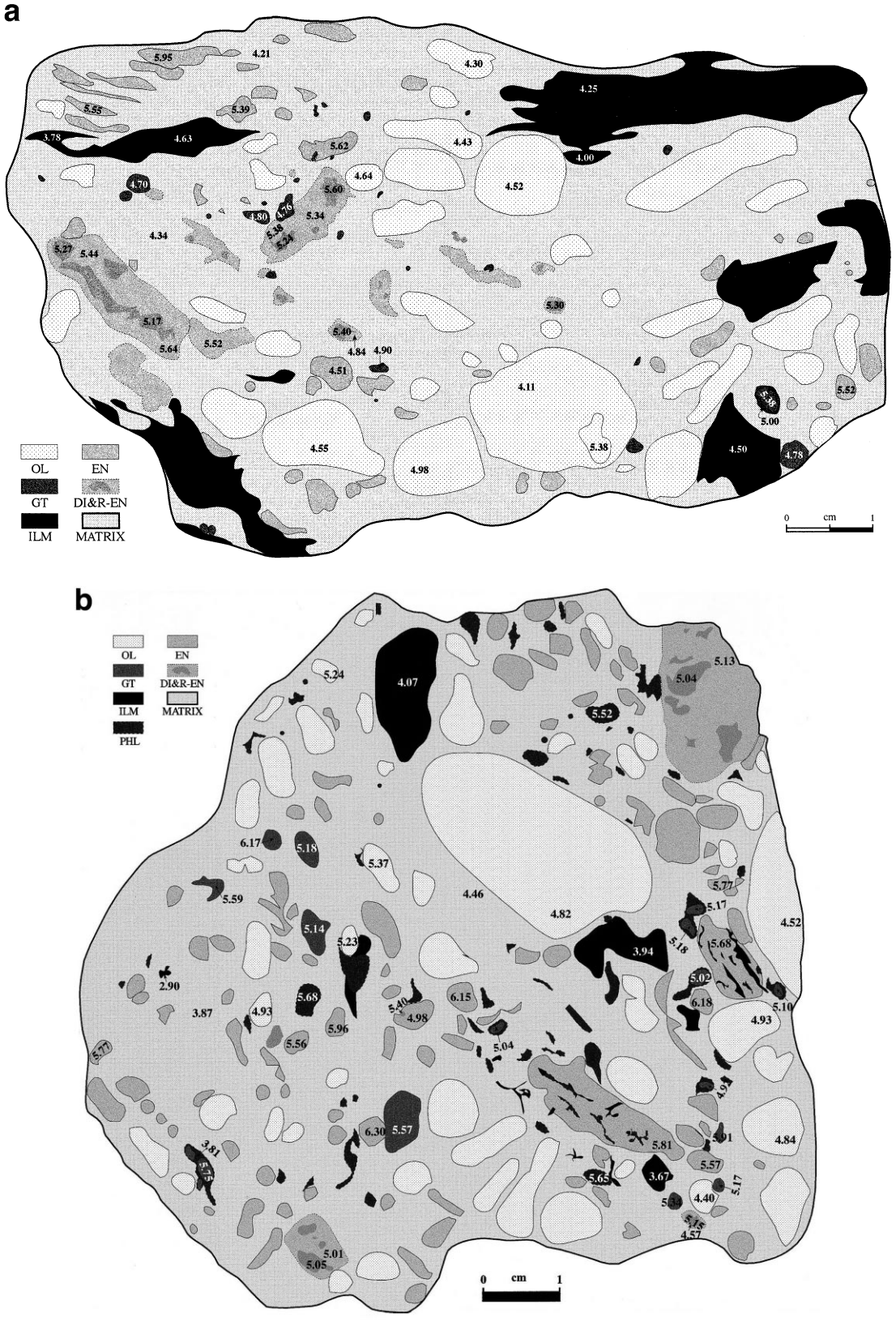
a
OL
EN
GT
DI&R-EN
ILM
MATRIX
0 cm 1
b
OL
EN
GT
DI&R-EN
ILM
MATRIX
PHL
0 cm 1

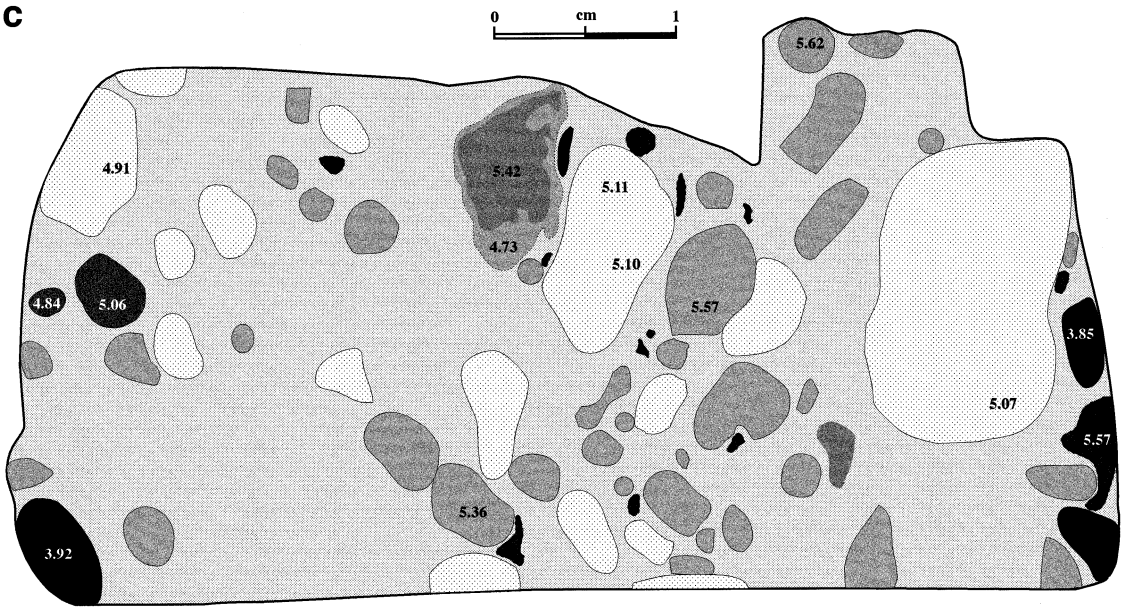

Fig. 1. Kimberley polymict xenoliths and oxygen isotope distribution in minerals (per mil). The scale bar = 1 cm. (a) JJG1414; (b) BD2394; (c) BD344; (d) BD2666 (overleaf).

years. Metasomatic enrichment is evident in the trace element and radiogenic isotope geochemistry of minerals from kimberlite-borne mantle xenoliths and diamond inclusions - a consequence of the migration of melts from sub-lithospheric sources [1–13].

Unequivocal evidence of melt interaction is occasionally preserved in xenoliths and these play a critical role in understanding mantle evolution [14–19]. Geochemical evidence of melt interaction is primarily detectable in phases that have a high concentration of trace elements and/or radiogenic isotopes such as clinopyroxene and amphibole. Oxygen isotopes also respond to melt interaction and in low temperature environments provide a powerful means of understanding these processes [20–22]. However, under mantle conditions, universally high temperatures limit the magnitude of oxygen isotopic fractionation and favour equilibrium, such that local oxygen isotope variation induced by melt interaction will be a subtle, and in all probability, a relatively short term phenomenon.

Knowledge of the oxygen isotope composition of the mantle [23] has been significantly influenced by new data generated using laser-assisted fluorination techniques [19,24–27]. The key feature of laser heating is that efficient extraction of oxygen from refractory minerals means that $\delta^{18}O$ values can be determined to a higher precision. Uncertainties in oxygen isotope data for refractory minerals obtained by conventional methods implied that the mantle was locally heterogeneous with respect to $\delta^{18}O$, with values of component minerals extending from +4.5 to +7.2‰ [28]. These data concur with the prevailing $\delta^{18}O$ evidence from basalts that a degree of oxygen isotope heterogeneity existed in the mantle [29] and were interpreted as either being a result of high temperature fractionation reversals or of open-system fluid interaction (see discussion in [25]).

However, laser-assisted fluorination analyses of mantle minerals have clearly shown that mantle peridotites possess only a narrow range of $\delta^{18}O$ values [25,30] despite the reports of heterogeneity in oxygen by conventional methods. The $\delta^{18}O$ values of over 100 samples of olivine in spinel-garnet- and diamond-facies peridotites are almost

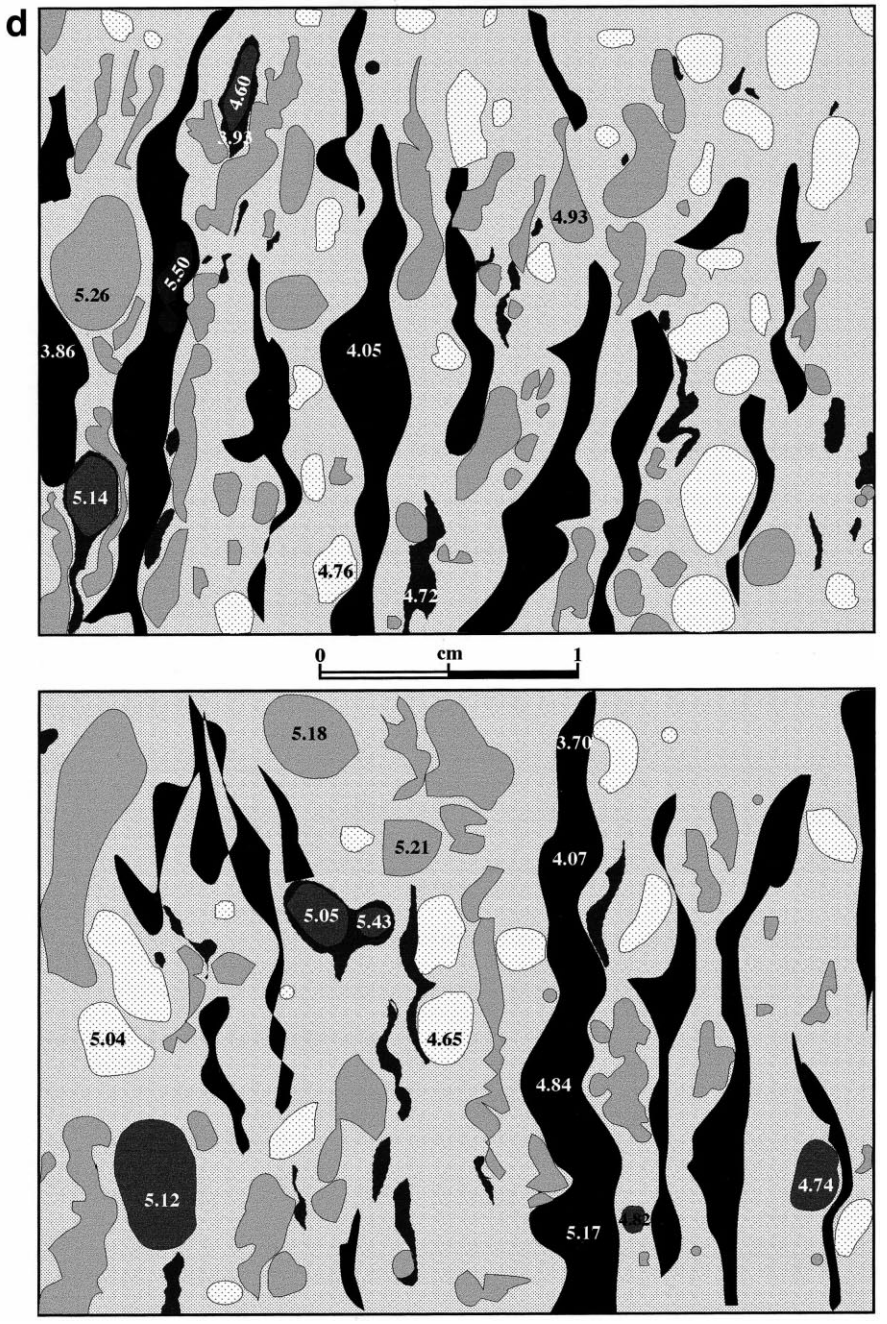

Fig. 1 (*continued*).

invariant, averaging 5.2 ± 0.3‰ with no evidence for significant isotopic disequilibrium in ordinary peridotite lithologies.

In this paper we report oxygen isotope data for mineral assemblages in highly unusual Kimberley polymict xenoliths, South Africa, which show petrographic evidence of fluid-related deformation and brecciation.

Table 1
Oxygen isotopes of minerals from the polymict xenoliths, South Africa

Mineral	Texture	$\delta^{18}O$	Mineral	Texture	$\delta^{18}O$
JJG1414					
Olivine	Porpyroclastic	4.30	Enstatite	Porphyroclastic	5.52
Olivine	Porpyroclastic	4.51	Enstatite	Porphyroclastic	5.55
Olivine	Porpyroclastic	4.52	Enstatite	Porphyroclastic	5.62
Olivine	Porpyroclastic	4.55	Enstatite	Porphyroclastic	5.95
Olivine	Porpyroclastic	4.64	Enstatite	Rim*	4.84
Olivine	Porpyroclastic	4.98	Enstatite	Rim	5.34
Olivine	Porpyroclastic	5.38	Enstatite	Rim	5.38
Olivine	Neoblastic*	4.34	Enstatite	Rim	5.44
Olivine	Neoblastic*	4.21	Enstatite	Rim	5.64
Olivine	Neoblastic*	4.11	Diopside	Porphyroclastic	5.17
Garnet	Pink, core	5.38	Diopside	Porphyroclastic	5.24
Garnet	Orange, rim*	5.00	Diopside	Porphyroclastic	5.27
Garnet	Orange	4.70	Diopside	Porphyroclastic	5.30
Garnet	Brown	4.76	Diopside	Porphyroclastic	5.40
Garnet	Brown	4.80	Diopside	Porphyroclastic	5.60
Garnet	Purple	4.78	Ilmenite	Discrete, core	4.63
Garnet	Purple	4.90	Ilmenite	Discrete, rim	3.78
Garnet	Lilac	5.17	Ilmenite	Discrete, core	4.25
Enstatite	Porphyroclastic	5.39	Ilmenite	Discrete, rim	4.00
Enstatite	Porphyroclastic	5.52	Ilmenite	Discrete, core	4.50
BD2394					
Olivine	Coarse	4.40	Enstatite	Coarse	5.56
Olivine	Coarse	4.52	Enstatite	Coarse	5.57
Olivine	Coarse	4.82	Enstatite	Coarse	5.77
Olivine	Coarse	4.84	Enstatite	Coarse	5.77
Olivine	Coarse	4.93	Enstatite	Coarse	5.96
Olivine	Coarse	4.93	Enstatite	Coarse	6.15
Olivine	Coarse	5.23	Enstatite	Coarse	6.18
Olivine	Coarse	5.24	Enstatite	Coarse	6.30
Olivine	Coarse	5.37	Enstatite	Coarse[a]	4.98
Olivine	Intergranular*	4.46	Enstatite	Rim*	4.57
Olivine	Intergranular*	3.87	Enstatite	Rim	5.01
Garnet	Colourless	5.10	Enstatite	Rim	5.13
Garnet	Yellowish pink	5.02	Diopside	Coarse	5.04
Garnet	Yellowish pink	5.18	Diopside	Coarse	5.05
Garnet	Yellowish pink	5.91	Diopside	Coarse	5.15
Garnet	Yellowish pink	6.17	Diopside	Secondary*	5.40
Garnet	Pink	5.18	Phlogopite	Primary	5.65
Garnet	Pink	5.57	Phlogopite	Primary	5.68
Garnet	Pink	5.75	Phlogopite	Secondary	5.52
Garnet	Orange	5.34	Phlogopite	Secondary*[b]	3.81
Garnet	Brown	5.59	Ilmenite	Coarse	4.23
Garnet	Purple	4.92	Ilmenite	Coarse	4.07
Garnet	Purple	5.17	Ilmenite	Coarse	3.94
Garnet	Claret	5.04	Ilmenite	Small	3.67
Garnet	Lilac	5.14	Ilmenite	Tiny[c]	2.90
Garnet	Lilac	5.17			
BD344					
Olivine	Coarse	4.91	Enstatite	Coarse	5.57
Olivine	Coarse	5.07	Enstatite	Coarse	5.62
Olivine	Coarse	5.10	Enstatite	Rim	4.73
Olivine	Coarse	5.11	Diopside	Coarse	5.42

Table 1 (*continued*)

Mineral	Texture	$\delta^{18}O$	Mineral	Texture	$\delta^{18}O$
Garnet	Purple	4.84	Phlogopite	Secondary	5.57
Garnet	Claret	5.06	Ilmenite	Coarse	3.92
Enstatite	Coarse	5.36	Ilmenite	Small	3.85
BD2666					
Olivine	Coarse	4.65	Garnet	Claret	5.43
Olivine	Coarse	4.76	Enstatite	Coarse	4.93
Olivine	Coarse	4.95	Enstatite	Coarse	5.17
Olivine	Coarse	5.04	Enstatite	Coarse	5.18
Olivine	Coarse	5.05	Enstatite	Coarse	5.21
Garnet	Pink	5.05	Enstatite	Coarse	5.26
Garnet	Pink	5.12	Enstatite	Coarse	5.47
Garnet	Pink	5.14	Phlogopite	Secondary	5.50
Garnet	Purple	4.60	Phlogopite	Secondary	4.72
Garnet	Purple	4.74	Phlogopite	Secondary*[b]	3.93
Garnet	Purple	4.90	Ilmenite	Vein	4.05
Garnet	Purple	4.92	Ilmenite	Vein	3.86
Garnet	Purple	5.06	Ilmenite	Vein 1	3.70
Garnet	Purple	5.09	Ilmenite	Vein 2	4.09
Garnet	Lilac	4.82	Ilmenite	Vein 3	4.84
Garnet	Lilac	5.06	Ilmenite	Vein 4	5.17

The data marked by an asterisk (*) are obtained by mass balance in which smaller minerals were added to a mineral whose oxygen isotope was known and the final isotope composition was calculated from the measured value. This method was also used for neoblastic olivine aggregates and tiny phlogopite aggregates but serpentine between grains was impossible to remove. In such cases the oxygen isotopic composition of the neoblastic or intergranular olivine was calibrated from the measured value by subtraction of the estimated modal percentage of serpentine. The serpentine $\delta^{18}O$ was determined from two analyses of separated grains and gave a value of 2.5‰.

[a]Enstatite replaced by a secondary diopside.

[b]Tiny secondary phlogopite aggregates (+serpentine+ilmenite) replacing garnet.

[c]Tiny ilmenite overgrown with sulphide.

2. Polymict peridotites JJG1414, BD2394, BD344 and BD2666

Four polymict peridotite breccias from Kimberley were obtained for this study (Fig. 1a–d). These polymict xenoliths are clinopyroxene-poor (0–3%) harzburgites and consist of a wide variety of 'lithologies' and 'minerals' together with ilmenite and phlogopite [31,32]. Polymict rock (JJG1414) is strongly deformed and contains porphyroclastic olivine, enstatite, diopside, garnet, and ilmenite set in a dark green neoblastic olivine matrix. Polymict peridotites (BD2394, BD344 and BD2666) are less deformed granular rocks composed of olivine and enstatite with minor garnet and diopside set in intergranular fine-grain olivine, secondary phlogopite with ilmenite veins. All the coarse diopsides in the polymict rocks have brown enstatite rims, partially or completely replacing the host diopside. Replacement is usually accompanied by the formation of finely disseminated opaque minerals. The grain boundaries between the diopside and enstatite rim are poorly defined and the rim enstatites are sheared. The only secondary diopside found in BD2394 clearly replaces enstatite. Micas occur as reddish-golden brown phlogopite, large irregular dark brown phlogopite interstitial to other minerals, and tiny euhedral phlogopite aggregates replacing garnet, olivine, enstatite, diopside. On this basis the former can be thought of as 'primary' and the latter as 'secondary'. Ilmenites from JJG1414 display a well-equilibrated, polygranular mosaic texture and 120° triple junctions are common in the core. Ilmenites from BD2394 and BD344 occur in different forms. Ilmenites in BD2666 occur as a quantity of irregular ilmenite layers or veinlets.

3. Sample preparation and analytical technique

A transverse slice of each polymict peridotite was cut into a mosaic of thin-section slices which were doubly polished to ca 500 μm thickness (Fig. 1). Following electron- and ion-microprobe studies, the coatings were removed and the slices were held onto glass plates using double-sided sticky tape. Selected areas of the wafer were carefully fractured and mineral fragments were removed, examined for purity under the binocular microscope, and cleaned with acetone in an ultrasonic bath for 20 min. The mass of each sample required for analysis is approximately 1.5 mg (silicates) and 2 mg (oxides) giving a spatial resolution of <1 mm for isotope mapping of thin sections. The majority of oxygen isotope analyses were made on two or more fragments of the same grain in order to ascertain the extent of oxygen isotope heterogeneity.

Minerals were analysed using the laser fluorination technique [24,33]. Two laser-fluorination systems, using either Nd-YAG and CO_2 lasers to heat samples in the presence of BrF_5, were used for oxygen isotope analyses. The Nd-YAG system described by Mattey and Macpherson [24] produces oxygen which is converted to carbon dioxide over hot graphite for isotope analysis as CO_2 gas. The automated CO_2 laser system [33] operates in a similar manner other than that isotope ratios are measured directly on oxygen gas. Minerals of all types were run on both systems for which oxygen yields and the precision and accuracy of oxygen isotope data were indistinguishable. Oxygen yields greater than 97% were obtained for all the minerals presented in this paper. Data quality was monitored using a range of internal standards to correct for within-run offsets and each batch of data were then normalised to the mean value obtained for NBS-30 biotite (+5.10‰). Day-to-day

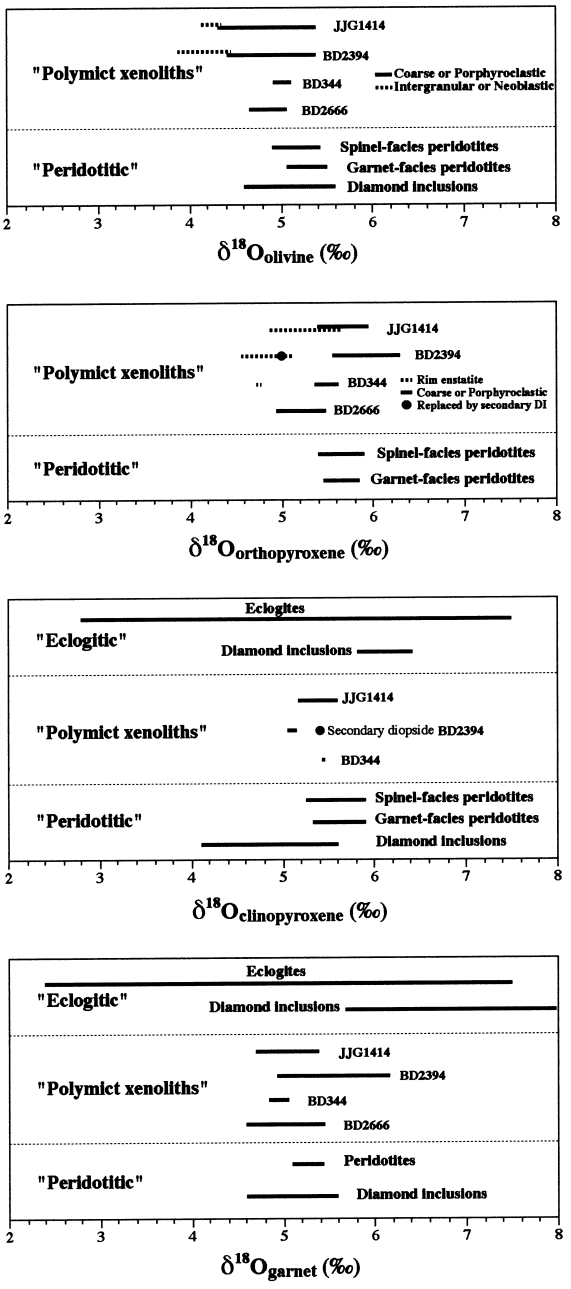

←

Fig. 2. Oxygen isotope composition of olivine, orthopyroxene, clinopyroxene and garnet from the Kimberley polymict xenoliths, South Africa. Note that coarse, porphyroclastic relic minerals have higher $\delta^{18}O$ ratios that are closer to the 'average mantle' value than intergranular or neoblastic phases and minerals occurring as reaction rims. In addition note that the range in $\delta^{18}O$ is similar to that reported from a huge range of wet and dry, cold and hot, sheared and granular mantle rocks (spinel, garnet and diamond facies) comparative data for minerals from P-type diamond inclusions and peridotites, as well as E-type diamond inclusions and eclogites worldwide, are from several sources. [25,30,36,37].

corrections are typically less than ±0.2‰. All corrected data are reported in permil relative to V-SMOW. Reproducibility of data for SC olivine (4.86‰), [24], QBLC quartz (8.88‰), [34], and Gore Mountain Garnet (+5.80‰), [35] were in the order of ±0.15‰ (2σ), although replicate analyses of samples were usually reproducible to better than 0.1‰.

4. Results

Oxygen isotope ratios for minerals from the polymict xenoliths are given in Table 1 and the range in individual mineral phases is plotted in Figs. 2 and 3.

4.1. Olivine

Oxygen isotope ratios in olivines exhibit a large variation and the dominant grains have a lower $\delta^{18}O$ ratio than that of olivines from garnet-facies

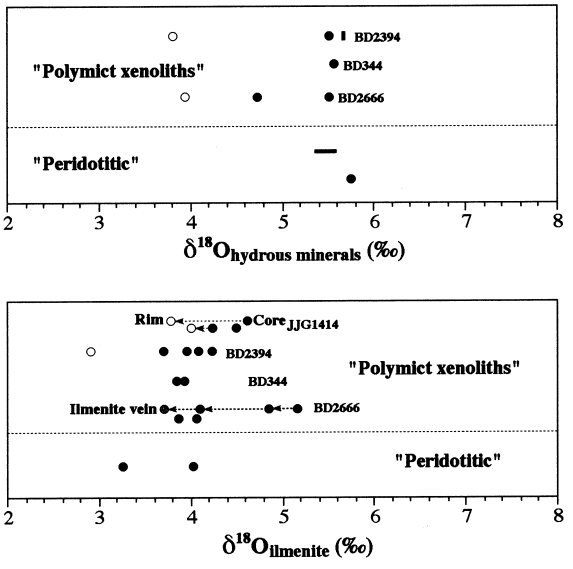

Fig. 3. Oxygen isotope compositions in phlogopite and ilmenite from the Kimberley polymict xenoliths, South Africa. Note that these K and Ti rich phases which may be 'secondary' in origin have lower $\delta^{18}O$ than the minerals in Fig. 2 which could be presumed to be 'primary'. Also they differ from the 'average mantle' value of 5.2. Comparative data are taken from several sources [19,24–26,30].

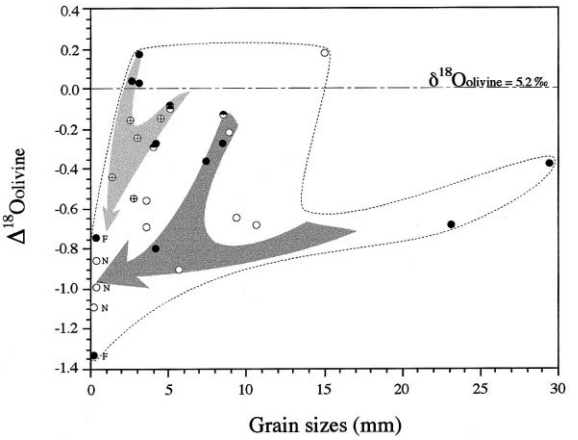

Fig. 4. Oxygen isotope correlation with grain size in olivines from the Kimberley polymict xenoliths. $\Delta^{18}O_{olivine} = \delta^{18}O_{olivine}$ (‰)−5.2. Note that the finer grained (F) or neoblastic (N) olivines have lower $\delta^{18}O$ ratios than average mantle and larger mineral grains (i.e., filled and half filled circles). Note that the coarser grained olivine porphyroclasts have retained a $\delta^{18}O$ ratio equivalent to the 'average mantle' (5.2‰). The average oxygen isotope value for olivines from garnet-facies mantle xenoliths worldwide is 5.2 [25,30,37]. (NB: Filled circle BD2394; open circle JJG1414; half filled circle BD344; crossed circle BD 2666.)

mantle xenoliths world-wide with a few analyses falling in that range (Fig. 2). The range in $\delta^{18}O$ (>1‰) is broadly equivalent to the range for mantle olivines (i.e., diamond-facies to spinel-facies, anhydrous and hydrous mantle, low and high temperature, granular and sheared peridotites) reflecting a complex origin and the existence of oxygen isotope disequilibrium [25,30,36,37]. Relative to the porphyroclastic or coarse olivines, neoblastic or fine-grained intergranular olivines show low $\delta^{18}O < 4.5$‰ (Fig. 4). The lowest $\delta^{18}O$ measured in olivine was from a very fine grained olivine which may have important information about the processes and the temperatures that affected these olivines. In addition the most forsteritic, coarsest olivines tend to have the highest $\delta^{18}O$ values (Fig. 4) broadly equivalent to the average mantle value of Mattey et al. [25,30]. One can infer that the formation of less forsteritic, neoblastic olivines was inextricably linked to a process that produced lower oxygen isotope ratios with a relatively higher iron content.

4.2. Garnet

Garnets from the polymict xenoliths broadly display a similar oxygen isotope signature as those from P-type diamond inclusions and peridotites world-wide (Fig. 2). The relatively restricted range and the lack of extreme $\delta^{18}O$ in garnets from polymict peridotites perhaps excludes any petrogenetic link to eclogitic parageneses (i.e., E-type diamond inclusions and eclogites) as these are normally characterised by a much wider range in $\delta^{18}O$. Relative to the peridotitic garnets, garnets from the polymict xenoliths show a larger $\delta^{18}O$ range and many analyses have a lower $\delta^{18}O$ than the low limit for peridotitic garnets. One polymict rock (BD2394) is distinguished from the others in that garnets in this rock exhibit a larger range ($>1.2‰$) in $\delta^{18}O$ and some grains have much higher $\delta^{18}O$ (up to 6.17‰) than peridotitic garnets [25,30,36,37]. In general terms the red, high chromium garnets tend to have lower $\delta^{18}O$ than the pink, low chromium garnets.

4.3. Enstatite

Enstatites in the polymict xenoliths also show a larger $\delta^{18}O$ variation than mantle peridotites world-wide (Fig. 2), like the olivines and garnets. The dominant porphyroclastic and coarse enstatites (Fig. 5) fall within, or beyond, the mantle $\delta^{18}O$ array except for BD2666 whose enstatites have a lower oxygen isotope signature than those from mantle peridotites. The larger range and much higher $\delta^{18}O$ signature, observed in enstatites from BD2394, are also recorded in olivines and garnets (Fig. 2). The rim enstatites are extremely depleted in ^{18}O relative to the porphyroclastic and coarse enstatites from the same rock. This may indicate that disequilibrium is preserved between rim enstatites and porphyroclastic or coarse enstatites as well as diopsides surrounded by enstatites. A coarse enstatite replaced by secondary diopside from BD2394 has a very low $\delta^{18}O$. The process of rim enstatite formation records a process that led to the conversion of clinopyroxene to orthopyroxene (i.e., lherzolite to harzburgite protolith) and a lowering of the oxygen isotope composition.

4.4. Diopside

Diopsides in polymict xenoliths have a similar isotope signature to diopsides from peridotites on a worldwide scale, particularly those from spinel- and garnet-facies peridotites. Coarse diopsides, from the polymict xenolith BD2394, exhibit an extremely low and homogeneous isotope signature

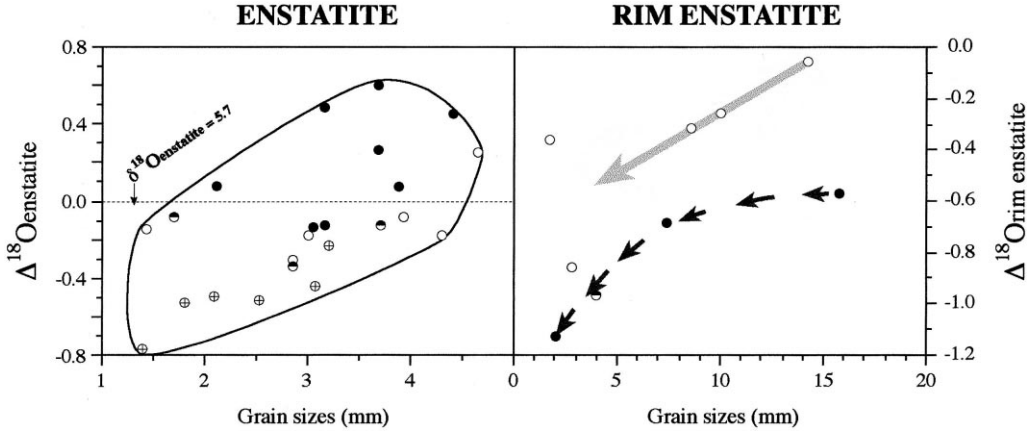

Fig. 5. Oxygen isotope correlation with the grain sizes in enstatites from the Kimberley polymict xenoliths. As in the case of olivine the coarse enstatites have retained a $\delta^{18}O$ equivalent to 'average mantle'. Core enstatite and rim enstatite deviate from the mantle value moreso if they are fine grained than coarse grained. $\Delta^{18}O_{enstatite}$ reflects the oxygen isotope differentiation in polymict enstatites relative to the average value of enstatites from garnet-facies mantle xenoliths worldwide ($\delta^{18}O = 5.7‰$), [25,30,37]. (NB: Filled circle BD2394; open circle JJG1414; half filled circle BD 344; crossed circle BD 2666.)

(Table 1 and Fig. 2). This contrasts markedly with other coarse mineral phases (i.e. olivine, enstatite and garnet) so that the oxygen isotope fractionation between diopside and enstatite plots outside the mantle peridotite field. A secondary diopside from this rock shows much higher $\delta^{18}O$ than the coarse diopside (Table 1 and Fig. 2). However the coarse enstatite replaced by this secondary diopside has a lower $\delta^{18}O$ than all other coarse enstatites. Porphyroclastic diopside from JJG1414 displays a relative higher $\delta^{18}O$ and larger isotope range in $\delta^{18}O$. Oxygen isotope fractionation between diopside and porphyroclastic enstatite overlaps with the mantle field worldwide [32]. However, the oxygen isotope fractionation between core diopside and rim enstatite pairs from all the polymict xenoliths plots in low $\delta^{18}O$ area and does not overlap with the mantle peridotitic field [19,25,30,38].

4.5. Phlogopite

Phlogopites from the polymict xenoliths show a low oxygen isotope ratio relative to phlogopite from garnet-facies peridotite [30] and the $\delta^{18}O$ value varies remarkably between different grain size groups (Fig. 3). Large 'primary' phlogopites have the highest $\delta^{18}O$, similar to amphibole and mica from spinel- and garnet-facies peridotites. Large irregular phlogopites show a higher $\delta^{18}O$ than the small subhedral or euhedral phlogopite (secondary?). Three analyses of phlogopite from three different polymict rocks have very similar $\delta^{18}O$ (Fig. 3), in turn similar to that reported from garnet-facies peridotite. Tiny euhedral phlogopite aggregates from BD2394 and BD2666 are exceedingly depleted in ^{18}O ($\delta^{18}O < 3‰$) and their association with minor ilmenite and serpentine may point to a secondary origin. Melt ingress that led to the growth of euhedral phlogopite has lowered the oxygen isotope ratio.

4.6. Ilmenite

$\delta^{18}O$ in these polymict ilmenites varies considerably between different samples (Fig. 3). Coarse ilmenites from BD2394 and BD344 show a higher $\delta^{18}O$ than smaller grains. An ilmenite overgrown with sulphide from BD2394 has an extremely low $\delta^{18}O$ ($< 3‰$) whilst ilmenite from a vein in BD2666 has a range in $\delta^{18}O$ that extends to higher oxygen isotope ratios ($> 5.0‰$). The core in the porphyroclastic ilmenite from JJG1414 is more enriched in ^{18}O than the rim with the maximum fractionation between the core to the rim of $> 0.8‰$, which corresponds to the major element variation. An ilmenite vein from BD2666 shows a systematic variation in $\delta^{18}O$ along the length of the vein. This is consistent with the elemental variation such as Cr_2O_3 [32]. More than $1.4‰$ $\delta^{18}O$ fractionation in ca 2 cm distance may indicate oxygen isotope disequilibrium. Analyses from the centre of a wider vein show a similar $\delta^{18}O$ as coarse ilmenite from BD2394 and BD344, the core of porphyroclastic ilmenite from JJG1414, and an ilmenite from a garnet facies peridotite (Fig. 3). In general terms fine grained, high chromium ilmenite has a light $\delta^{18}O$ and coarse low chromium ilmenite has a heavy $\delta^{18}O$, perhaps a result of fluid processes.

5. Discussion

5.1. Oxygen isotope disequilibrium and $\delta^{18}O$ fractionation

Olivines from the polymict xenoliths have a range in $\delta^{18}O$ which overlaps with the range observed in spinel-, garnet-, and diamond-facies mantle peridotites (Fig. 2). This suggests that such olivines may in part be related to a peridotite precursor, but as the $\delta^{18}O$ range of polymict olivines extends to values as low as $+4‰$ some olivine has been modified by more complex processes. The most forsteritic olivines have $\delta^{18}O$ values similar to the average for worldwide mantle ($+5.2‰$), [25] but the correlation between $\delta^{18}O$ and Fo content (Fig. 6) indicates that the change toward lower $\delta^{18}O$ values is associated with iron enrichment. Similarly, $\delta^{18}O$ values for orthopyroxenes, clinopyroxenes and garnets overlap with the normal range observed in mantle peridotites, but the range in $\delta^{18}O$ exhibited by polymict minerals extends to lower, and in some

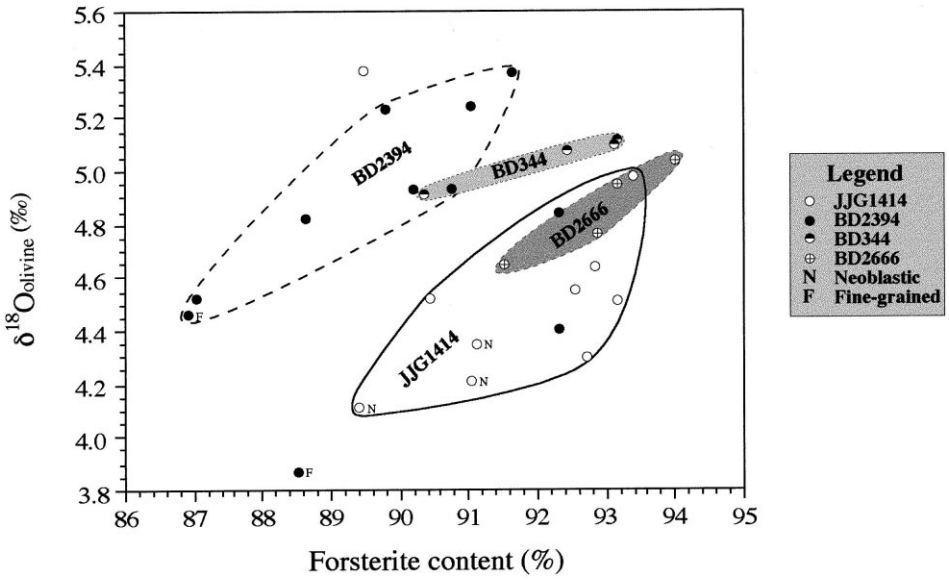

Fig. 6. Oxygen isotope ratio and forsterite content of olivines from the Kimberley polymict xenoliths. Note that fine-grained (F), neoblastic (N) olivines tend to have lower $\delta^{18}O$ ratios than coarse grained, forsteritic olivines that in the majority of cases closely approach the 'average mantle' value. Forsterite content equals 100 Mg/(Mg+Fe) atomic ratio. Overall an increase in fayalite content (i.e., iron enrichment) in olivine is associated with a decrease in $\delta^{18}O$ ratio. (NB: Filled circle BD2394; open circle JJG1414; half filled circle BD344; crossed circle BD 2666.)

cases, higher $\delta^{18}O$ values. Thus all the minerals in these polymict xenoliths preserve varying degrees of oxygen isotope disequilibrium which is characterised by local $\delta^{18}O$ depletion (and, less commonly, enrichment) relative to normal peridotite.

The development of oxygen isotope disequilibrium can be related to texture with fine-grain neoblastic or intergranular olivines and porphyroclastic or coarse olivines (JJG1414 and BD2394) commonly exhibiting low disequilibrium $\delta^{18}O$ values (Table 1 and Fig. 2). Coexisting olivine, orthopyroxene and clinopyroxene in texturally equilibrated mantle peridotites exhibit positive $\Delta^{18}O_{opx-ol}$, $\Delta_{18}O_{cpx-ol}$ and $\Delta^{18}O_{opx-cpx}$ fractionation averaging 0.4‰, 0.5‰ and 0.1‰, respectively, which are consistent with isotopic equilibrium at normal mantle conditions [25]. Negative $\Delta^{18}O_{opx-ol}$ fractionation in rim-enstatite (JJG1414, BD2394 and BD344) and coarse enstatite (BD2666) illustrates that $\delta^{18}O$ disequilibrium exists between two phases that are dominant in polymict xenoliths. Inter-granular $\delta^{18}O$ disequilibrium is also shown by the pyroxenes. $\Delta^{18}O_{Cpx-coarse\ opx}$ and $\Delta^{18}O_{cpx\ rim-opx\ pairs}$ (BD2394) and the dominant diopside-rim enstatite pairs plot outside the normal mantle field [19,25,30,37,38] away from the equilibrated fractionation band.

5.2. Fluid migration, deformation and mineral zonation

Petrographical and geochemical studies show that polymict xenoliths were affected by complex processes [31] involving episodes of metasomatism [32,39,40]. The latter may be the reason for the large range in oxygen isotopes in the constituent minerals. As already mentioned, olivines with more Fe enrichment tend toward more depletion in ^{18}O (Fig. 6), and oxygen isotopes in polymict garnets show systematic variations with major and trace element compositions (Fig. 7). However garnets with low $\delta^{18}O$ ratios, high LREE and Nb tend to be enriched in chromium and calcium and may reflect a mixture of provenance and metasomatic process. Lowry et al. [26] report that high Cr subcalcic garnets from diamondiferous peridotites and occurring as syngenetic diamond inclu-

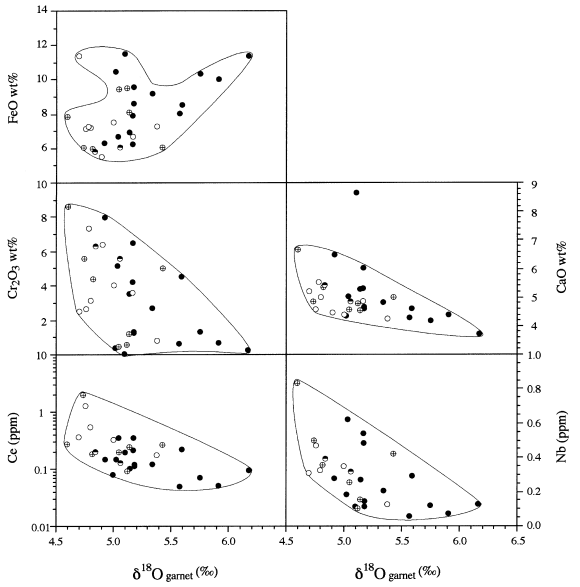

Fig. 7. Oxygen isotope and major and trace element variation in garnets from the Kimberley polymict xenoliths. Note that garnets with $\delta^{18}O$ ratios proximal to 'average mantle' tend to be depleted in Cr, Ca, Ce and Nb whereas those garnets with $\delta^{18}O$ most distal from the 'average mantle' value can be enriched in Cr, Ca, Ce and Nb. A decrease in $\delta^{18}O$ is accompanied by an increase in Cr, Ca, the LREE and Nb in enstatite. (NB: Filled circle BD2394; open circle JJG1414; half filled circle BD 344; crossed circle BD 2666.)

sions generally possess lower $\delta^{18}O$ values than low Cr garnets. Mechanisms that could create garnets with a low $\delta^{18}O$ signature may be a reaction or phase transformation involving low $\delta^{18}O$ phase that produces garnet or isotopic exchange with a low $\delta^{18}O$ fluid or melt [26]. Some polymict garnets share the characteristics of diamond facies garnets from deep cratonic peridotites, but polymict peridotites contain low $\delta^{18}O$, LREE enriched garnets that are both Cr-rich and Ca-rich. If one were to invoke fluid processes as a mechanism then this would explain the LREE enrichment and the low $\delta^{18}O$ but the Cr–Ca systematics would require an unusual melt composition or an alternative/additional explanation.

If we attempt to understand these compositional variations in the garnets in terms of mantle rocks it is evident that all the garnets from the polymict peridotites have Ca–Cr variations consistent with a lherzolite precursor, not harzburgite or dunite. However, the similarity to a lherzolite precursor is complex in that the garnets display enough compositional variation so as to straddle the variation shown by discrete nodules, granular lherzolites and sheared lherzolites. In general the high Cr garnets, which are compositionally similar to those found in sheared lherzolites, have low $\delta^{18}O$ ratios and the low Cr garnets, which are compositionally similar to those found in discrete nodules/granular lherzolites, have high $\delta^{18}O$ ratios. So perhaps the Ca–Cr–O relationships relate to a complex interplay between the mineralogy of

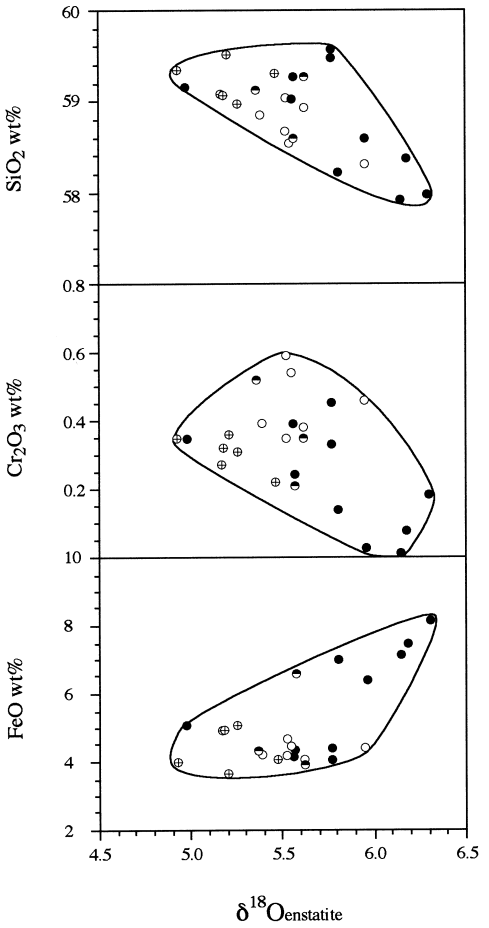

Fig. 8. Oxygen isotope correlation with major element concentrations in porphyroclastic or coarse enstatites from the Kimberley polymict xenoliths. A decrease in $\delta^{18}O$ in enstatites is accompanied by a decrease in Fe and an increase in Cr and Si. (NB: Filled circle BD2394; open circle JJG1414; half filled circle BD 344; crossed circle BD 2666.)

the precursor and the inextricable link between melt transfer and deformation.

The covariance of $\delta^{18}O$ with major and trace element concentrations is also apparent in pyroxenes from the Kimberley polymict xenoliths (Fig. 6 and Fig. 7). The negative correlation between $\delta^{18}O$ and Cr_2O_3 and SiO_2 in porphyroclastic or coarse enstatite (Fig. 8) and the negative correlation between $\delta^{18}O$ and FeO, SiO_2 and Zr in rim enstatite and diopside (Fig. 9) illustrates that the $\delta^{18}O$ depletion may accompany the conversion of lherzolite to harzburgite resulting from the influx of low $\delta^{18}O$, iron- and silica-rich melts. No correlation between the $\delta^{18}O$ and rare earth element abundance exists in rim enstatite and diopside. While the $\delta^{18}O$ depletion is accompanied by an enrichment in Zr in rim enstatite and diopside the Zr/Hf remains constant (Fig. 9).

Taking all these observations together indicates that melt migration not only leads to large elemental heterogeneity but also to a low oxygen isotope signature in grains that have texturally re-equilibrated. We suggest that the large oxygen isotope variation and fractionation between, and within the constituent minerals of these polymict xenoliths, is a result of melt interaction and textural reequilibration that has been arrested after entrainment and eruption in kimberlite magma. This has effectively frozen the developing oxygen disequilibrium phenomena in time.

While the composition of the melts may be complex, generally speaking they appear to be enriched in the LREE, Nb, Fe, Ti, Si, Ca, to have a constant Zr/Hf and to have low $\delta^{18}O$. Tiny euhedral secondary phlogopites and small ilmenites (Fig. 3) which also have the lowest oxygen isotope ratios may also point to the melt being K and Ti-rich and rather unique if ilmenite is a primary crystallisation product. The oxygen isotope exchange between precursor minerals and melts in these polymict xenoliths may be consistent with open-system exchange [41,42].

Oxygen isotope disequilibrium generated by open-system melt interaction is a transient phenomena that reequilibrates rapidly under mantle conditions by diffusion. Transport distances for oxygen by self diffusion in garnet [43] are in excess of 1 mm within a million years at mantle

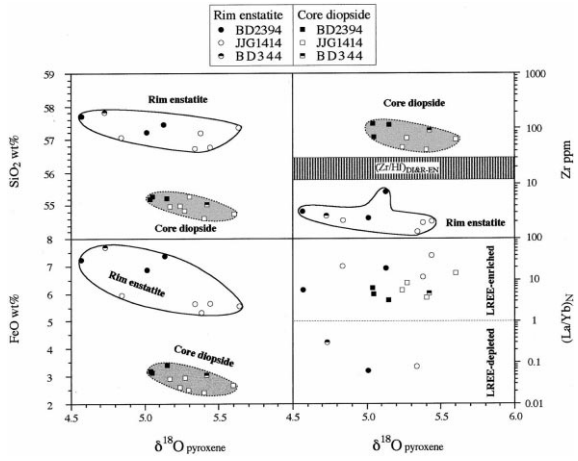

Fig. 9. Oxygen isotope covariance with major and REE element concentrations in rim enstatites and diopsides from the Kimberley polymict xenoliths. Rim enstatites have lower $\delta^{18}O$ than core diopsides and the reaction is associated with an increase in Fe and Si. (NB: Filled circle BD2394; open circle JJG1414; half filled circle BD 344; crossed circle BD 2666.)

temperatures, such that grains will lose oxygen isotopic heterogeneity after a relatively short period. Presence of grain boundary fluid and deformation processes do not favour preservation of isotopic disequilibrium and an alternative possibility is that the metasomatism is a very recent event and that it was terminated by the entrainment and eruption process as a result of quenching. This provides a mechanism to preserve disequilibrium in the minerals of the polymict xenoliths and may be analogous to the preservation of similar oxygen isotope disequilibrium in P-type diamond inclusions [26,37]. In either case, it indicates that the oxygen isotope disequilibrium retained within these polymict xenoliths may represent a phenomenon localised along a propagating fracture in the lithosphere where displacement led to the juxtaposition of diverse lithologies. Deformation along that crack may be assisted by the preferential passage of melts, eventually leading to the crack/conduit acting as a site of entrainment of mantle material.

Another noticeable point is that the broadly positive correlation between FeO content and oxygen isotope ratios exist in polymict garnets

(Fig. 5) and enstatites (Fig. 6). This appears to be enigmatic in that iron enrichment would normally be associated with melt processes and a lowering of the oxygen isotopic composition. The more depleted minerals (i.e. high MgO, Cr_2O_3 garnets and low CaO enstatites) are presumably from depleted protoliths. These protoliths (e.g. low calcium, garnet harzburgite) are preferentially affected by metasomatic melts which impart a low oxygen isotope signature. In contrast the growth of rim enstatite and diopside shows an FeO enrichment (Fig. 7) and a low oxygen isotope ratio. They may indicate that the rim enstatite formed from a low $\delta^{18}O$, Fe- and Si-rich melt (e.g. hydrothermal fluid?). Thus the diverse elemental and oxygen isotopic behaviour in different minerals in the polymict xenoliths may illustrate that different fluids affected different minerals most logically prior to their juxtaposition in the polymict peridotite.

Apart from the metasomatic effects, the general correlation between oxygen isotopes and grain sizes in olivines (Fig. 8) as well as the excellent positive correlation between $\delta^{18}O$ and grain sizes in enstatites (Fig. 9) suggests that melt-related diffusion may also affect the polymict xenoliths perhaps as an integral part of the melt infiltration process (i.e. fluid-assisted deformation). Minerals with smaller grain sizes tend to be more depleted in ^{18}O because inter-mineral oxygen isotope diffusion or $\delta^{18}O$ exchange between minerals and a fluid are more likely to affect these grains. In contrast, the large minerals (e.g. olivine, enstatite, garnet) have retained evidence of their pre-existent provenance which in most cases was a peridotitic paragenesis.

6. Conclusions

1. All the mineral phases in the polymict xenoliths show a large inter-mineral disequilibrium in oxygen isotopes and have low $\delta^{18}O$ values relative to equivalent minerals in mantle xenoliths from elsewhere. Some minerals (i.e. garnet, ilmenite and diopside) still show intra-mineral $\delta^{18}O$ disequilibrium. Normally the reaction rim has a lower $\delta^{18}O$ value than the core of the mineral.
2. A decrease in $\delta^{18}O$ ratio is accompanied by changes in mineral chemistry: an increase in Fe in olivine; an increase in Cr, Ca, the LREE and Nb in enstatite, and an increase in Cr and Si in enstatite. If melt migration is the main process resulting in the inter- and intra-mineral disequilibrium and the low $\delta^{18}O$ ratios then the melts are enriched in Fe, Cr, Ca, Si, the LREE and Nb
3. Some minerals have retained information about the precursory lithologies (harzburgite/lherzolite) that were disrupted during the deformation process that juxtaposed such chemically and isotopically diverse minerals. It is envisaged that this may have occurred during crack propagation part of the continuum that eventually leads to explosive entrainment.
4. Oxygen isotope ratios in many of the minerals from the polymict xenoliths are similar to a large variety of mantle rocks stable in the spinel, garnet and diamond stability fields, i.e., sheared and granular lherzolites, hot and cold peridotites, discrete nodules, wet and dry peridotites. No unequivocal evidence exists for the presence of an eclogite precursor or minerals of eclogitic paragenesis.

Acknowledgements

Financial support for this project is acknowledged from the Overseas Research Student Scheme (UK) and the K.C. Wong Education Foundation (Hong Kong). This paper is part of the doctoral thesis of H.Z. We thank Graham Pearson for his comments on an earlier version. Francis Albarede is thanked for his work in finding reviewers and Simon Sheppard and U. Weichert for their careful reviews.*[FA]*

References

[1] M.A. Menzies, R.V. Murthy, Enriched mantle: Nd and Sr isotopes in diopsides from kimberlite nodules, Nature 283 (1980) 634–636.

[2] J.D. Kramers, C.B. Smith, N.P. Lock, R.S. Harmon, F.R. Boyd, Can kimberlites be generated from an ordinary mantle?, Nature 291 (1981) 53–56.
[3] J.D. Kramers, J.C.M. Roddick, J.B. Dawson, Trace element and isotope studies on veined, metasomatic and 'MARID' xenoliths from Bultfontein, Southern Africa, Earth Planet. Sci. Lett. 65 (1983) 90–106.
[4] S.H. Richardson, J.J. Gurney, A.J. Erlank, J.W. Harris, Origins of diamonds in old enriched mantle, Nature 310 (1984) 198–202.
[5] S.H. Richardson, A.J. Erlank, H. SR, Kimberlite-borne garnet peridotite xenoliths from old enriched subcontinental lithosphere, Earth Planet. Sci. Lett. 75 (1985) 116–128.
[6] S.H. Richardson, J.W. Harris, J.J. Gurney, Three generations of diamonds from old continental mantle, Nature 366 (1993) 256–258.
[7] A.J. Erlank, F.G. Waters, C.J. Hawkesworth, S.E. Haggerty, H.L. Allsopp, R.S. Rickard, M.A. Menzies, Evidence for mantle metasomatism in peridotite nodules from Kimberley pipes, South Africa, in: M.A. Menzies, C.J. Hawkesworth (Eds.), Mantle Metasomatism, Academic Press Geology Series (1987) 221–309.
[8] B. Harte, P.A. Winterburn, J.J. Gurney, Metasomatic and enrichment phenomena in garnet peridotite facies mantle xenoliths from the Matsoku kimberlite pipe, Lesotho, in: M.A. Menzies, C.J. Hawkesworth (Eds.), Mantle Metasomatism, Academic Press Geology Series (1987) 145–220.
[9] R.J. Walker, R.W. Carlson, S.B. Shirey, B. FB, Os, Sr, Nd, and Pb isotope systematics of southern African peridotites xenoliths: Implications for the chemical evolution of subcontinental mantle, Geochim. Cosmochim. Acta 53 (1989) 1583–1595.
[10] C.J. Hawkesworth, A.J. Erlank, P.D. Kempton, F.G. Waters, Mantle metasomatism: Isotope and trace-element trends in xenoliths from Kimberley, south Africa, Chem. Geol. 85 (1990) 19–34.
[11] S.H. Richardson, Age and early evolution of the continental mantle, in: M.A. Menzies (Ed.), Continental Mantle, Clarendon Press, Oxford (1990) 55–65.
[12] D.G. Pearson, R.W. Carlson, S.B. Shirey, F.R. Boyd, P.H. Nixon, Stabilisation of Archaean lithospheric mantle: A Re–Os isotope study of peridotite xenoliths from the Kaapvaal craton, Earth Planet. Sci. Lett. 134 (1995) 341–357.
[13] V. Olive, R.M. Ellam, B. Harte, A Re–Os isotope study of ultramafic xenoliths from the Matsoku kimberlite, Earth Planet. Sci. Lett. 150 (1997) 129–140.
[14] G.M. Yaxley, A.J. Crawford, D.H. Green, Evidence for carbonatite metasomatism in spinel peridotite xenoliths from western Victoria, Earth Planet. Sci. Lett. 107 (1991) 305–317.
[15] E.H. Hauri, N. Shimizu, J.J. Dieu, S.R. Hart, Evidence for hot spot-related carbonatite metasomatism in the oceanic upper mantle, Nature 365 (1993) 221–227.
[16] R.L. Rudnick, W.F. McDonough, B.W. Chappell, Carbonatite metasomatism in the northern Tanzanian mantle, Earth Planet. Sci. Lett. 114 (1993) 463–475.
[17] D.A. Ionov, A.W. Hofmann, N. Shimizu, metasomatism-induced melting in mantle xenoliths from Mongolia, J. Petrol. 35 (1994a) 753–785.
[18] P. Schiano, R. Clocchiatti, Worldwide occurrence of silica-rich melts in sub-continental and sub-oceanic mantle minerals, Nature 368 (1994) 621–624.
[19] G. Chazot, D. Lowry, M.A. Menzies, D.P. Mattey, Oxygen isotope composition of hydrous and anhydrous mantle peridotites, Geochim. Cosmochim. Acta 61 (1997) 161–169.
[20] H.P. Taylor, S.M.F. Sheppard, Igneous rocks: I. Processes of isotopic fractionation and isotopic systematics, in: J.W. Valley, H.P. Taylor, J.R. O'Neil (Eds.), Stable Isotopes in High Temperature Geological Processes, Reviews in Mineralogy 16 (1986) 227–271.
[21] R.E. Criss, H.P. Taylor, Meteoric-hydrothermal systems, in: J.W. Valley, H.P. Taylor, J.R. O'Neil (Eds.), Stable Isotopes in High Temperature Geological Processes, Reviews in Mineralogy 16 (1986) 373–424.
[22] K. Muehlenbachs, Alteration of the oceanic crust and the ^{18}O history of seawater, in: J.W. Valley, H.P. Taylor, J.R. O'Neil (Eds.), Stable Isotopes in High Temperature Geological Processes, Reviews in Mineralogy 16 (1986) 425–444.
[23] M. Javoy, $^{18}O/^{16}O$ and D/H ratios in high temperature peridotites, Colloques International du CRNS 272 (1980) 279–287.
[24] D. Mattey, C. Macpherson, High-precision oxygen isotope microanalysis of ferromagnesian minerals by laser-fluorination, Chem. Geol. 105 (1993) 305–318.
[25] D.P. Mattey, D. Lowry, C.G. Macpherson, Oxygen isotope composition of mantle peridotite, Earth Planet. Sci. Lett. 128 (1994) 231–241.
[26] D. Lowry, D.P. Mattey, J.W. Harris, Oxygen isotope composition of syngenetic inclusions in diamond from the Finsch Mine, RSA, Geochim. Cosmochim. Acta 63 (1999) 1825–1836.
[27] J.M. Eiler, K.A. Farley, J.W. Valley, E. Hauri, H. Craig, S.R. Hart, E.M. Stolper, Oxygen isotope variations in ocean island basalt phenocrysts, Geochim. Cosmochim. Acta 61 (1997) 2281–2293.
[28] T.K. Kyser, Stable isotopes in the continental lithospheric mantle, in: M.A. Menzies (Ed.), Continental Mantle, Clarendon Press, Oxford (1990) 127–156.
[29] R.S. Harmon, J. Hoefs, Oxygen isotope heterogeneity of the mantle deduced from global ^{18}O systematics of basalts from different geotectonic settings, Contrib. Mineral. Petrol. 120 (1995) 95–114.
[30] D.P. Mattey, D. Lowry, C.G. Macpherson, G. Chazot, Oxygen isotope composition of mantle minerals by laser fluorination analysis: homogeneity in peridotites, heterogeneity in eclogites, Mineral. Mag. Ext. Abstr. 58A (1994) 573–574.
[31] P.J. Lawless, J.J. Gurney, J.B. Dawson, Polymict peridotites from the Bultfontein and De Beers mines, Kimberley, South Africa. The mantle sample: inclusions in kimberlites and other volcanics, Proceedings of the Second In-

ternational Kimberlite Conference, Volume 2 (1979) 145–155.

[32] H.-F. Zhang, Petrology and geochemistry of on- and off-craton mantle rocks: eastern China and southern Africa, Ph.D. Thesis, Royal Holloway, University of London, 1998, 183 pp.

[33] D.P. Mattey, LaserPrep: An Automatic Laser-Fluorination System for Micromass 'Optima' or 'Prism' Mass Spectrometers, Micromass UK Limited, Manchester, 1997, 6 pp.

[34] N. Grassineau, Contribution des isotopes stables de l'oxygene et de l'hydrogene a l'etude d'un grand complexe volcanique d'arc: Example de l'arc du kamchatka, C.E.I., Ph.D. Thesis, Universite de Paris 7, 1994, 293 pp.

[35] J.W. Valley, N. Kitchen, M.J. Kohn, C.R. Niendorf, M.J. Spicuzza, Strategies for high precision oxygen isotope analysis by laser fluorination, Geochim. Cosmochim. Acta 59 (1995) 5223–5231.

[36] D. Lowry, D.P. Mattey, C.G. Macpherson, J.W. Harris, Oxygen isotope variations among peridotitic and eclogitic syngenetic inclusions in diamond, Terra Abstr. 5 (1993) 375.

[37] D. Lowry, D.P. Mattey, C.G. Macpherson, J.W. Harris, Evidence for stable isotope and chemical disequilibrium associated with diamond formation in the mantle., Mineral. Mag. Ext. Abstr. 58A (1994) 535–536.

[38] Y.-G. Xu, M.A. Menzies, D.P. Mattey, D. Lowry, B. Harte, R.W. Hinton, The nature of the lithospheric mantle near the Tancheng-Lujiang fault, China: an integration of texture, chemistry and O-isotopes, Chem. Geol. 134 (1996) 67–81.

[39] L. Morfi, B. Harte, P. Hill, J. Gurney, Polymict peridotites - a link between deformed peridotites and megacry its from komberlites, Ofioliti 24 (1a) (1999) 134.

[40] H.F. Zhang, D.P. Mattey, N. Grassineau, D. Lowry, M. Brownless, J.J. Gurney, M.A. Menzies, Recent fluid processes in the Kaaprael craton, South Africa: oxygen isotope disequilibrium in polymict peridotite breccias, Ofioliti 24 (1a) (1999) 194.

[41] R.T. Gregory, R.E. Criss, Isotopic exchange in open and closed systems, in: J.W. Valley, H.P. Taylor, J.R. O'Neil (Eds.), Stable Isotopes in High Temperature Geological Processes, Reviews in Mineralogy 16 (1986) 91–127.

[42] R.T. Gregory, R.E. Criss, H.P.J. Taylor, Oxygen isotope exchange kinetics of mineral pairs in closed and open systems: applications to problems of hydrothermal alteration of igneous rocks and Precambrian iron formations, Chem. Geol. 75 (1989) 1–42.

[43] Y.F. Zheng, Calculation of oxygen isotope fractionation in anhydrous silicate minerals, Geochim. Cosmochim. Acta 57 (1993) 1079–1091.